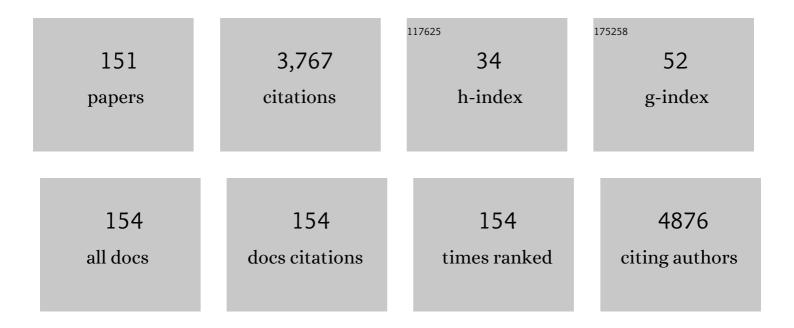
Guglielmo G Condorelli

List of Publications by Year in descending order

Source: https://exaly.com/author-pdf/529628/publications.pdf Version: 2024-02-01



#	Article	IF	CITATIONS
1	Elusive Presence of Chloride in Mixed Halide Perovskite Solar Cells. Journal of Physical Chemistry Letters, 2014, 5, 3532-3538.	4.6	175
2	Cyclic fatigue of different nickel-titanium endodontic rotary instruments. Oral Surgery Oral Medicine Oral Pathology Oral Radiology and Endodontics, 2006, 102, e106-e114.	1.4	126
3	Magnetic behaviour of TbPc2 single-molecule magnets chemically grafted on silicon surface. Nature Communications, 2014, 5, 4582.	12.8	115
4	Anchoring Molecular Magnets on the Si(100) Surface. Angewandte Chemie - International Edition, 2004, 43, 4081-4084.	13.8	101
5	Engineering of molecular architectures of β-diketonate precursors toward new advanced materials. Coordination Chemistry Reviews, 2007, 251, 1931-1950.	18.8	91
6	Shaping Ability of Four Nickel-Titanium Rotary Instruments in Simulated S-Shaped Canals. Journal of Endodontics, 2009, 35, 883-886.	3.1	87
7	Similar Structural Dynamics for the Degradation of CH ₃ NH ₃ PbI ₃ in Air and in Vacuum. ChemPhysChem, 2015, 16, 3064-3071.	2.1	80
8	The effect of surface treatments of nickel-titanium files on wear and cutting efficiency. Oral Surgery Oral Medicine Oral Pathology Oral Radiology and Endodontics, 2000, 89, 363-368.	1.4	78
9	Highly reproducible ideal SiC Schottky rectifiers: effects of surface preparation and thermal annealing on the Ni/6H-SiC barrier height. Applied Physics A: Materials Science and Processing, 2003, 77, 827-833.	2.3	77
10	Photochemical Mechanism of the Formation of Nanometer-Sized Copper by UV Irradiation of Ethanol Bis(2,4-pentandionato)copper(II) Solutions. Chemistry of Materials, 2004, 16, 1260-1266.	6.7	68
11	Local Magnetic Properties of a Monolayer of Mn12 Single Molecule Magnets. Nano Letters, 2007, 7, 1551-1555.	9.1	68
12	Wear of Nickel-Titanium Endodontic Instruments Evaluated by Scanning Electron Microscopy: Effect of Ion Implantation. Journal of Endodontics, 2001, 27, 588-592.	3.1	62
13	Au–Ag/CeO2 and Au–Cu/CeO2 Catalysts for Volatile Organic Compounds Oxidation and CO Preferential Oxidation. Catalysis Letters, 2015, 145, 1691-1702.	2.6	62
14	Exclusive recognition of sarcosine in water and urine by a cavitand-functionalized silicon surface. Proceedings of the National Academy of Sciences of the United States of America, 2012, 109, 2263-2268.	7.1	61
15	Molecular Recognition on a Cavitand-Functionalized Silicon Surface. Journal of the American Chemical Society, 2009, 131, 7447-7455.	13.7	58
16	A single photochemical route for the formation of both copper nanoparticles and patterned nanostructured films. Journal of Materials Chemistry, 2003, 13, 2409-2411.	6.7	52
17	Cyclodextrin Anchoring on Magnetic Fe ₃ O ₄ Nanoparticles Modified with Phosphonic Linkers. European Journal of Inorganic Chemistry, 2012, 2012, 5323-5331.	2.0	52
18	Selective oxidation of CO in H2-rich stream over gold/iron oxide: An insight on the effect of catalyst pretreatment. Journal of Molecular Catalysis A, 2008, 284, 24-32.	4.8	51

#	Article	IF	CITATIONS
19	Cavitandâ€Grafted Silicon Microcantilevers as a Universal Probe for Illicit and Designer Drugs in Water. Angewandte Chemie - International Edition, 2014, 53, 9183-9188.	13.8	49
20	Effect of sterilization on the cutting efficiency of rotary nickel-titanium endodontic files. Oral Surgery Oral Medicine Oral Pathology Oral Radiology and Endodontics, 1999, 88, 343-347.	1.4	48
21	Defects in GT Rotary Instruments After Use: An SEM Study. Journal of Endodontics, 2001, 27, 782-785.	3.1	48
22	Site-Specific Anchoring of Tetrairon(III) Single Molecule Magnets on Functionalized Si(100) Surfaces. Chemistry of Materials, 2008, 20, 2405-2411.	6.7	47
23	Nanoparticles of Sr(OH)2: synthesis in homogeneous phase at low temperature and application for cultural heritage artefacts. Applied Physics A: Materials Science and Processing, 2008, 92, 137-141.	2.3	45
24	Spectroscopic and Theoretical Study of the Grafting Modes of Phosphonic Acids on ZnO Nanorods. Journal of Physical Chemistry C, 2013, 117, 5364-5372.	3.1	45
25	Surface segregation of Sb in doped TiO2 rutile. Applied Surface Science, 1995, 90, 289-295.	6.1	41
26	An x-ray photoelectron spectra and atomic force microscopy characterization of silica substrates engineered with a covalently assembled siloxane monolayer. Nanotechnology, 2005, 16, 2170-2175.	2.6	41
27	Grafting Cavitands on the Si(100) Surface. Langmuir, 2006, 22, 11126-11133.	3.5	41
28	Reversible photoswitching of stimuli-responsive Si(100) surfaces engineered with an assembled 1-cyano-1-phenyl-2-[4′-(10-undecenyloxy)phenyl]-ethylene monolayer. Journal of Materials Chemistry, 2008, 18, 5011.	6.7	41
29	Engineered Silica Surfaces with an Assembled C60Fullerene Monolayer. Chemistry of Materials, 2005, 17, 1079-1084.	6.7	39
30	Pitting Corrosion Resistance of Nickel–Titanium Rotary Instruments with Different Surface Treatments in Seventeen Percent Ethylenediaminetetraacetic Acid and Sodium Chloride Solutions. Journal of Endodontics, 2008, 34, 208-211.	3.1	39
31	Improvement of the fatigue resistance of NiTi endodontic files by surface and bulk modifications. International Endodontic Journal, 2010, 43, 866-873.	5.0	37
32	Self-Assembly of Nanosize Coordination Cages on Si(100) Surfaces. Chemistry - A European Journal, 2007, 13, 6891-6898.	3.3	36
33	Tunable luminescent properties of a europium complex monolayer. Journal of Materials Chemistry, 2009, 19, 3507.	6.7	36
34	Cavitand-Functionalized Porous Silicon as an Active Surface for Organophosphorus Vapor Detection. Langmuir, 2012, 28, 1782-1789.	3.5	36
35	Texture of MAPbI ₃ Layers Assisted by Chloride on Flat TiO ₂ Substrates. Journal of Physical Chemistry C, 2015, 119, 19808-19816.	3.1	36
36	MOCVD of Bismuth Oxides:Â Transport Properties and Deposition Mechanisms of the Bi(C6H5)3Precursor. Chemistry of Materials, 2004, 16, 3176-3183.	6.7	34

#	Article	IF	CITATIONS
37	Functionalization of PEGylated Fe3O4 magnetic nanoparticles with tetraphosphonate cavitand for biomedical application. Nanoscale, 2013, 5, 11438.	5.6	34
38	Multi-Scale-Porosity TiO2 scaffolds grown by innovative sputtering methods for high throughput hybrid photovoltaics. Scientific Reports, 2016, 6, 39509.	3.3	34
39	The early oxynitridation stages of hydrogen-terminated (100) silicon after exposure to N2:N2O. III. Initial conditions. Applied Physics A: Materials Science and Processing, 2003, 77, 403-409.	2.3	33
40	Viable Synthetic Route for a Luminescent Porphyrin Monolayer Covalently Assembled on a Molecularly Engineered Si(100) Surface. Chemistry of Materials, 2007, 19, 5102-5109.	6.7	33
41	AlN texturing and piezoelectricity on flexible substrates for sensor applications. Applied Physics Letters, 2015, 106, .	3.3	33
42	Metal-Organic Chemical Vapor Deposition of Copper-Containing Phases: Kinetics and Reaction Mechanisms. Chemistry of Materials, 1994, 6, 1861-1866.	6.7	32
43	Novel Photoactive Self-Assembled Monolayer for Immobilization and Cleavage of DNA. Langmuir, 2003, 19, 536-539.	3.5	32
44	Praseodymium Silicate as a High-kDielectric Candidate: An Insight into the Pr2O3-Film/Si-Substrate Interface Fabricated Through a Metal-Organic Chemical Vapor Deposition Process. Advanced Functional Materials, 2005, 15, 838-845.	14.9	32
45	Implications of TiO ₂ surface functionalization on polycrystalline mixed halide perovskite films and photovoltaic devices. Journal of Materials Chemistry A, 2015, 3, 20811-20818.	10.3	31
46	In situ synthesis of photoluminescent films of PVC, doped with Ce3+ ion. Journal of Photochemistry and Photobiology A: Chemistry, 2008, 195, 215-222.	3.9	30
47	Efficiency Enhancement in ZnO:Al-Based Dye-Sensitized Solar Cells Structured with Sputtered TiO ₂ Blocking Layers. Journal of Physical Chemistry C, 2014, 118, 6576-6585.	3.1	29
48	In-Situ Gas-Phase FTIR Monitoring of MOCVD Processes: LaF3 Films Using the Second Generation La(hfac)3·diglyme Precursor. Chemical Vapor Deposition, 2000, 6, 185-192.	1.3	28
49	Dye-Sensitizing of Self-Nanostructured Ti(:Zn)O ₂ /AZO Transparent Electrodes by Self-Assembly of 5,10,15,20-Tetrakis(4-carboxyphenyl)porphyrin. Journal of Physical Chemistry C, 2011, 115, 7760-7767.	3.1	28
50	Micro- and nanoscale electrical characterization of large-area graphene transferred to functional substrates. Beilstein Journal of Nanotechnology, 2013, 4, 234-242.	2.8	28
51	Density Control of Dodecamanganese Clusters Anchored on Silicon(100). Chemistry - A European Journal, 2006, 12, 3558-3566.	3.3	26
52	From Pbl ₂ to MAPbl ₃ through Layered Intermediates. Journal of Physical Chemistry C, 2016, 120, 19768-19777.	3.1	26
53	Fabrication Of Hard Coatings On NiTi Instruments. Journal of Endodontics, 2003, 29, 132-134.	3.1	25
54	Depositions of Nitrogen on NiTi Instruments. Journal of Endodontics, 2002, 28, 497-500.	3.1	24

#	Article	IF	CITATIONS
55	Chemical Analysis of Nickel-Titanium Rotary Instruments with and without Electropolishing after Cleaning Procedures with Sodium Hypochlorite. Journal of Endodontics, 2008, 34, 1391-1395.	3.1	23
56	Molecular recognition of halogen-tagged aromatic VOCs at the air–silicon interface. Chemical Communications, 2010, 46, 288-290.	4.1	23
57	Functionalization of atomically flat, dihydrogen terminated, (1 0 0) silicon via reaction with 1-alkyne. Applied Surface Science, 2005, 246, 52-67.	6.1	22
58	Study of the Anchoring Process of Tethered Unsymmetrical Zn-Phthalocyanines on TiO ₂ Nanostructured Thin Films. Journal of Physical Chemistry C, 2013, 117, 11176-11185.	3.1	22
59	X-ray photoemission spectroscopy study at different takeoff angles of hydrosilation of 1-alkynes at hydrogen-terminated 1A—1-reconstructed (100)-oriented silicon. Materials Science and Engineering C, 2003, 23, 989-994.	7.3	21
60	Enantioselective extraction mediated by a chiral cavitand–salen covalently assembled on a porous silicon surface. Chemical Communications, 2014, 50, 4993-4996.	4.1	21
61	Metal-Organic Chemical Vapor Deposition of Copper and Copper(I) Oxide: Kinetics and Reaction Mechanisms in the Presence of Oxygen. Chemistry of Materials, 1995, 7, 2096-2103.	6.7	20
62	Multifunctional magnetic nanoparticles for enhanced intracellular drug transport. Journal of Materials Chemistry B, 2015, 3, 4134-4145.	5.8	20
63	Growth of epitaxial TlBaCaCuO a-axis oriented films on LaAlO3 buffer layers grown on SrTiO3 (100) substrates. Journal of Alloys and Compounds, 1997, 251, 314-317.	5.5	19
64	Effect of Baî—,Caî—,Cu precursor matrix on the formation and properties of superconducting Tl2Ba2Canâ^`1CunOx films A combined metalorganic chemical vapour deposition and thallium vapour diffusion approach. Journal of Alloys and Compounds, 1997, 251, 332-336.	5.5	19
65	Engineered Si(100) surfaces for the gas-phase anchoring of metal β-diketonate complexes. Inorganica Chimica Acta, 2007, 360, 170-178.	2.4	19
66	Hierarchical Route for the Fabrication of Cavitand-Modified Nanostructured ZnO Fibers for Volatile Organic Compound Detection. Journal of Physical Chemistry C, 2016, 120, 12611-12617.	3.1	19
67	Comparison Between Folic Acid and gH625 Peptide-Based Functionalization of Fe3O4 Magnetic Nanoparticles for Enhanced Cell Internalization. Nanoscale Research Letters, 2018, 13, 45.	5.7	19
68	Kinetic Study of MOCVD Fabrication of Copper(I) and Copper(II) Oxide Films. Chemical Vapor Deposition, 1999, 5, 21-27.	1.3	18
69	Nucleation and Growth of Copper Oxide Films in MOCVD Processes Using the β-Ketoiminate Precursor 4,4′-(1,2-Ethanediyldinitrilo)bis(2-pentanonate) Copper(II). Chemical Vapor Deposition, 1999, 5, 237-244.	1.3	18
70	MOCVD of YF3 and Y1-xErxF3 Thin Films from Precursors Synthesized In Situ. Chemical Vapor Deposition, 2005, 11, 324-329.	1.3	18
71	Reproducible synthesis by metal-organic chemical vapour deposition and thallium vapour diffusion of oriented thin-films : intergrowth of and structures. Superconductor Science and Technology, 1996, 9, 570-577.	3.5	17
72	X-ray-photoemission-spectroscopy evidence for anomalous oxidation states of silicon after exposure of hydrogen-terminated single-crystalline (100) silicon to a diluted N2 : N2O atmosphere. Journal Physics D: Applied Physics, 2002, 35, 1032-1038.	2.8	17

#	Article	IF	CITATIONS
73	MOCVD of LaAlO3 Films from a Molten Precursor Mixture: Characterization of Liquid, Gas, and Deposited Phases. Chemical Vapor Deposition, 2004, 10, 171-177.	1.3	17
74	Multistep Anchoring Route of Luminescent (5-Amino-1,10-phenanthroline)tris(dibenzoylmethane)europium(III) on Si(100). European Journal of Inorganic Chemistry, 2010, 2010, 4121-4129.	2.0	17
75	Selfâ€Assembly of TbPc ₂ Singleâ€Molecule Magnets on Surface through Multiple Hydrogen Bonding. Small, 2018, 14, 1702572.	10.0	17
76	Hybrid nickel-free graphene/porphyrin rings for photodegradation of emerging pollutants in water. RSC Advances, 2019, 9, 30182-30194.	3.6	17
77	Evidence for the precursors of nitrided silicon in the early stages of silicon oxynitridation in N2:N2O atmosphere. Applied Physics Letters, 2001, 79, 2378-2380.	3.3	16
78	MOCVD of Lanthanum Oxides from La(tmhd)3 and La(tmod)3 Precursors: A Thermal and Kinetic Investigation. Chemical Vapor Deposition, 2006, 12, 46-53.	1.3	16
79	Nickel nanostructured materials from liquid phase photodeposition. Journal of Nanoparticle Research, 2007, 9, 611-619.	1.9	16
80	Direct Growth on Si(100) of Isolated Octahedral Mil-101(Fe) Crystals for the Separation of Aromatic Vapors. Journal of Physical Chemistry C, 2019, 123, 28836-28845.	3.1	16
81	Photochemistry of bis(1,1,1,5,5,5-hexafluoro-2,4-pentanedionato)strontium tetraglyme solutions for eventual liquid phase photochemical deposition. Inorganica Chimica Acta, 2005, 358, 1873-1881.	2.4	15
82	A study by FTIR and mass spectroscopy of the decomposition of precursors for the MOCVD of high temperature superconductors. Journal of Alloys and Compounds, 1997, 251, 297-302.	5.5	14
83	Covalent Functionalization of Silicon Surfaces with a Cavitand-Modified Salen. European Journal of Inorganic Chemistry, 2011, 2011, 2124-2131.	2.0	14
84	Combined Strategy to Realize Efficient Photoelectrodes for Low Temperature Fabrication of Dye Solar Cells. ACS Applied Materials & Interfaces, 2014, 6, 6425-6433.	8.0	14
85	Characterization of a new fluorescence-enhancing substrate for microarrays with femtomolar sensitivity. Sensors and Actuators B: Chemical, 2014, 192, 15-22.	7.8	14
86	Low temperature sputtered TiO ₂ nano sheaths on electrospun PES fibers as high porosity photoactive material. RSC Advances, 2015, 5, 73444-73450.	3.6	14
87	Dual-Functional Nano-Functionalized Titanium Scaffolds to Inhibit Bacterial Growth and Enhance Osteointegration. Nanomaterials, 2021, 11, 2634.	4.1	14
88	Comparison of Thermal and Mass-Transport Properties of Bi(tmhd)3, Bi(p-tol)3, and Bi(o-tol)3 MOCVD Precursors. Chemical Vapor Deposition, 2005, 11, 261-268.	1.3	13
89	One pot grafting of tetrairon(III) single molecule magnets on silicon. Polyhedron, 2009, 28, 1758-1763.	2.2	13
90	Thermally induced structural modifications of nano-sized anatase films and the effects on the dye-TiO2 surface interactions. Applied Surface Science, 2014, 296, 69-78.	6.1	13

#	Article	IF	CITATIONS
91	MOCVD Growth of Perovskite Multiferroic BiFeO ₃ Films: The Effect of Doping at the A and/or B Sites on the Structural, Morphological and Ferroelectric Properties. Advanced Materials Interfaces, 2017, 4, 1601025.	3.7	13
92	Microscopic model for pH sensing mechanism in zinc-based nanowalls. Sensors and Actuators B: Chemical, 2019, 296, 126614.	7.8	13
93	Kinetics and Mechanisms of MOCVD Processes for the Fabrication of Sr-Containing Films From Sr(hfac)2Tetraglyme Precursor. Chemistry of Materials, 2002, 14, 4307-4312.	6.7	12
94	Piezoelectric domains in BiFeO3 films grown via MOCVD: Structure/property relationship. Surface and Coatings Technology, 2013, 230, 168-173.	4.8	12
95	Surface anchoring of bi-functional organic linkers on piezoelectric BiFeO 3 films and particles: Comparison between carboxylic and phosphonic tethering groups. Surface and Coatings Technology, 2018, 343, 75-82.	4.8	12
96	Combined IR and XPS characterization of organic refractory residues obtained by ion irradiation of simple icy mixtures. Astronomy and Astrophysics, 2018, 620, A123.	5.1	12
97	Synthesis of MIL-Modified Fe3O4 Magnetic Nanoparticles for Enhancing Uptake and Efficiency of Temozolomide in Glioblastoma Treatment. International Journal of Molecular Sciences, 2022, 23, 2874.	4.1	12
98	Fluorine-free and fluorine containing MOCVD precursors for electronic oxides: a comparison. Materials Science and Engineering B: Solid-State Materials for Advanced Technology, 2005, 118, 264-269.	3.5	11
99	Metal-Organic Chemical Vapor Deposition of Ferroelectric SrBi2Ta2O9Films from a Fluorine-Containing Precursor System. Chemistry of Materials, 2006, 18, 1016-1022.	6.7	11
100	Porphyrin functionalized bismuth ferrite for enhanced solar light photocatalysis. Dalton Transactions, 2020, 49, 8652-8660.	3.3	11
101	Piezoelectric BiFeO3 Thin Films: Optimization of MOCVD Process on Si. Nanomaterials, 2020, 10, 630.	4.1	11
102	In-situ Synthesis of the Anhydrous La(hfac)3 Precursor: A Viable Route to the MOCVD of LaF3. Chemical Vapor Deposition, 2001, 7, 151-156.	1.3	10
103	Self-Assembled Monolayers of Dipolar Nonlinear Optical Nickel(II) Molecules on the Si(100) Surface with Nanoscale Uniformity. Langmuir, 2006, 22, 7952-7955.	3.5	10
104	Metalâ€Organic Chemical Vapor Deposition (MOCVD) Synthesis of Heteroepitaxial Pr _{0.7} Ca _{0.3} MnO ₃ Films: Effects of Processing Conditions on Structural/Morphological and Functional Properties. ChemistryOpen, 2015, 4, 523-532.	1.9	10
105	MOCVD of Sr-Containing Oxides: Transport Properties and Deposition Mechanisms of the Sr(tmhd)2·pmdeta Precursor. Chemical Vapor Deposition, 2005, 11, 269-275.	1.3	9
106	BiFeO ₃ Films Doped in the A or B Sites: Effects on the Structural and Morphological Properties. Journal of Nanoscience and Nanotechnology, 2011, 11, 8221-8225.	0.9	9
107	In situ metalation of free base phthalocyanine covalently bonded to silicon surfaces. Beilstein Journal of Nanotechnology, 2014, 5, 2222-2229.	2.8	9
108	Early Growth Stages of Aluminum Oxide (Al ₂ O ₃) Insulating Layers by Thermal- and Plasma-Enhanced Atomic Layer Deposition on AlGaN/GaN Heterostructures. ACS Applied Electronic Materials, 2022, 4, 406-415.	4.3	9

#	Article	IF	CITATIONS
109	Morphology and surface properties of YBCO and TBCCO thin films: influence of etching processes. Physica C: Superconductivity and Its Applications, 1996, 271, 83-93.	1.2	8
110	The early oxynitridation stages of hydrogen-terminated (100) silicon after exposure to N 2 :N 2 O. Nitrogen bonding states. Applied Physics A: Materials Science and Processing, 2002, 75, 585-590.	2.3	8
111	Environment influence on Ti diffusion and layer degradation of a SiC/Ni[sub 2]Si/TiW/Au contact structure. Journal of Vacuum Science & Technology an Official Journal of the American Vacuum Society B, Microelectronics Processing and Phenomena, 2004, 22, 966.	1.6	8
112	Phaseâ€selective Route to Vâ€O Film Formation: A Systematic MOCVD Study Into the Effects of Deposition Temperature on Structure and Morphology. Chemical Vapor Deposition, 2015, 21, 319-326.	1.3	8
113	New Synthetic Route for the Growth of α-FeOOH/NH ₂ -Mil-101 Films on Copper Foil for High Surface Area Electrodes. ACS Omega, 2019, 4, 18495-18501.	3.5	8
114	Nitrogen doped spongy TiO2 layers for sensors application. Materials Science in Semiconductor Processing, 2019, 98, 44-48.	4.0	8
115	Piezoelectric Ba and Ti co-doped BiFeO ₃ textured films: selective growth of solid solutions or nanocomposites. Journal of Materials Chemistry C, 2020, 8, 16168-16179.	5.5	8
116	Synthesis and spectroscopic characterisation of MoO3thin films. Journal of Materials Chemistry, 1996, 6, 1335-1338.	6.7	7
117	Influence of growth mode on stoichiometry in epitaxial calcium ruthenate thin films. European Physical Journal B, 2004, 41, 3-9.	1.5	7
118	Core-electron x-ray photoelectron spectroscopy of the evolution of nearly flat, terraced, homogeneously H-terminatedSi(100)during prolonged exposure to air at room temperature. Physical Review B, 2006, 74, .	3.2	7
119	Spatially Confined Functionalization of Transparent NiO Thin Films with a Luminescent (1,10â€Phenanthroline)tris(2â€thenoyltrifluoroacetonato)europium Monolayer. European Journal of Inorganic Chemistry, 2015, 2015, 1261-1268.	2.0	7
120	Polymeric platform for the growth of chemically anchored ZnO nanostructures by ALD. RSC Advances, 2018, 8, 521-530.	3.6	7
121	Cavitand-Decorated Silicon Columnar Nanostructures for the Surface Recognition of Volatile Nitroaromatic Compounds. ACS Omega, 2018, 3, 9172-9181.	3.5	7
122	Heterogeneous growth of continuous ZIF-8 films on low-temperature amorphous silicon. Applied Surface Science, 2019, 473, 182-189.	6.1	7
123	Homogeneous and heterogeneous reactions in the decomposition of precursors for the MOCVD of high-k and ferroelectric films. Materials Science in Semiconductor Processing, 2002, 5, 135-139.	4.0	6
124	Precursor mutual interactions in the kinetics of MOCVD of SBT films. Materials Science in Semiconductor Processing, 2002, 5, 167-171.	4.0	6
125	Hierarchical Selfâ€Assembly of Luminescent Eu ^{III} Complexes on Silicon. European Journal of Inorganic Chemistry, 2014, 2014, 2687-2694.	2.0	6
126	Tetra-anionic porphyrin loading onto ZnO nanoneedles: A hybrid covalent/non covalent approach. Materials Chemistry and Physics, 2014, 143, 977-982.	4.0	6

#	Article	IF	CITATIONS
127	Effects of surface nature of different semiconductor substrates on the plasma enhanced atomic layer deposition growth of Al ₂ O ₃ gate dielectric thin films. Physica Status Solidi C: Current Topics in Solid State Physics, 2015, 12, 980-984.	0.8	6
128	A strategy to stabilise the local structure of Ti4+ and Zn2+ species against aging in TiO2/aluminium-doped ZnO bi-layers for applications in hybrid solar cells. Journal of Applied Physics, 2014, 116, .	2.5	5
129	Electrical and structural properties of Ti/Alâ€based contacts on AlGaN/GaN heterostructures with different quality. Physica Status Solidi (A) Applications and Materials Science, 2015, 212, 1091-1098.	1.8	5
130	Porous Gig-Lox TiO2 Doped with N2 at Room Temperature for P-Type Response to Ethanol. Chemosensors, 2019, 7, 12.	3.6	4
131	The Interplay between Fe3O4 Superparamagnetic Nanoparticles, Sodium Butyrate, and Folic Acid for Intracellular Transport. International Journal of Molecular Sciences, 2020, 21, 8473.	4.1	4
132	Dy-Doped BiFeO ₃ thin films: piezoelectric and bandgap tuning. Materials Advances, 2022, 3, 3446-3456.	5.4	4
133	TlBaCaCuO superconducting thin films via metal-organic chemical vapour deposition (MOCVD) and thallium vapour diffusion. Nuovo Cimento Della Societa Italiana Di Fisica D - Condensed Matter, Atomic, Molecular and Chemical Physics, Biophysics, 1994, 16, 1953-1959.	0.4	3
134	Structural and morphological properties of ultrathin YBCO films grown on single-crystal substrates. Nuovo Cimento Della Societa Italiana Di Fisica D - Condensed Matter, Atomic, Molecular and Chemical Physics, Biophysics, 1994, 16, 2031-2038.	0.4	3
135	Fabrication of TlBa2CaCu2O7c-Axis Oriented Films Through a Hybrid In-Situ MOCVD Process. Chemical Vapor Deposition, 2005, 11, 381-387.	1.3	3
136	Luminescent CeCl3 nanoparticles by Tris(1,1,1,5,5,5-hexafluoro-2,4-pentanedionato)cerium diglyme photolysis in chlorinated solvents. Inorganica Chimica Acta, 2006, 359, 4043-4052.	2.4	3
137	A practical MOCVD approach to the growth of Pr _{1-<i>x</i>} Ca <i>_x</i> MnO ₃ films on single crystal substrates. Physica Status Solidi (A) Applications and Materials Science, 2015, 212, 1550-1555.	1.8	3
138	The quest towards epitaxial BaMgF4 thin films: exploring MOCVD as a chemical scalable approach for the deposition of complex metal fluoride films. Dalton Transactions, 2016, 45, 17833-17842.	3.3	3
139	Selfâ€Poled Heteroepitaxial Bi _{(1â^'} <i>_x</i> ₎ Dy <i>_x</i> FeO ₃ Films with Promising Pyroelectric Properties. Advanced Materials Interfaces, 2022, 9, .	3.7	3
140	MOCVD Kinetics of Precursors for Ferroeletric SBT film. Materials Research Society Symposia Proceedings, 2000, 655, 352.	0.1	2
141	Bis(salicyladiminato)Ni(II) Schiff base complexes, grafted on H-terminated Si(100) surfaces, observed by Scanning Near-field Optical/Atomic Force Microscopy (SNOM/AFM). Physica Status Solidi C: Current Topics in Solid State Physics, 2005, 2, 4093-4096.	0.8	2
142	XPS, FTIR-ATR, and AFM Structural Study of Silicon-Grafted Triol Monolayers for Controlled Anchoring of Single Molecule Magnets. Journal of Physical Chemistry C, 2010, 114, 20696-20701.	3.1	2
143	Metal-Organic Chemical Vapor Deposition of BiFeO ₃ Based Multiferroics. Advances in Science and Technology, 0, , .	0.2	2
144	Chemical Engineering of Silicon with Functional Molecules. Science of Advanced Materials, 2011, 3, 362-377.	0.7	2

#	Article	IF	CITATIONS
145	Thermal and plasma-enhanced atomic layer deposition of hafnium oxide on semiconductor substrates. , 2014, , .		1
146	Multifunctional Magnetic Nanoparticles for Theranostic Applications. , 2018, , 335-370.		1
147	Effect of oxygen partial pressure on the Tl2Ba2CuOx→ Tl2Ba2CaCu2Oxtransformation. Journal of Materials Chemistry, 1996, 6, 1013-1017.	6.7	Ο
148	The Early Oxynitridation Stages of Hydrogen-Terminated Single-Crystalline Silicon in N2O Ambient. Materials Research Society Symposia Proceedings, 2000, 648, 1.	0.1	0
149	MOCVD Processes for Electronic Materials Adopting Bi(C6H5)3 Precursor. Materials Research Society Symposia Proceedings, 2004, 811, 231.	0.1	Ο
150	In Situ Monitoring of CVD for HTS Growth. , 1999, , 45-50.		0
151	Electroless Deposited IrOx Nanoparticles for Ni Foam Functionalization with Low Iridium Loading. ECS Meeting Abstracts, 2019	0.0	0